Available online at www.sciencedirect.com
SCIENCE DIRECT®
Journal of Nuclear Materials 337–339 (2005) 186–190
journal of nuclear materials
www.elsevier.com/locate/jnucmat

Three-dimensional proton trajectory analyses and simulation of neutral particle transport in an ICRF heated long pulse discharge on the large helical device

M. Shoji *, R. Kumazawa, K. Saito, T. Watanabe, Y. Nakamura, S. Masuzaki, S. Morita, M. Goto, N. Noda, N. Ohyabu, LHD Experimental Groups

National Institute for Fusion Science, Toki, 509-5292, Japan

Abstract

A three-dimensional neutral particle transport simulation code is applied to identify a source of the hydrogen outgas in a LHD long pulse discharge by ICRF heating. Radiation collapse induced by uncontrollable plasma density rise terminated the long pulse discharge. Toroidally non-uniform increases in the H_α emission and divertor temperature were observed. A CCD camera detected local heating of a vertically installed divertor plate, which is consistent with the strike points of the trajectories of protons accelerated by ICRF waves. The neutral particle transport simulation with the proton trajectory analyses shows that outgas from the divertor plates heated by the protons is necessary for explaining the observed toroidal non-uniform distribution of the H_α emission in the long pulse discharge.

PACS: 52.40.Hf
Keywords: DEGAS; ICRF; LHD; Neutrals; Steady state

1. Introduction

Plasma wall interaction in long pulse discharges is one of the critical issues in optimizing the first wall materials or the divertor design for future nuclear fusion reactors. The large helical device (LHD) has an advantage in long pulse discharge experiments due to the superconducting magnetic coils and plasma currentless operation [1]. We investigate the neutral particle transport induced by the plasma–wall interactions in LHD long pulse discharges heated by ion cyclotron range of frequency (ICRF). In the next section, the experimental set-up for the long pulse discharges is depicted, and the experimental results are shown in Section 3. Analyses on the proton trajectories and neutral particle transport are described in Sections 4 and 5, respectively. In the last section, we propose a possible solution for steady state plasma operation with the conclusion of this paper.

2. Experimental set-up for long pulse discharges

Fig. 1 gives a bird's eye view of the cross-section of the LHD vacuum vessel with plasma heating and diagnostic systems for long pulse discharges. The five kinds of vacuum ports (inner, outer, upper, lower and tangential ports) are equipped. Four divertor legs and ergodic

* Corresponding author.
E-mail address: shoji@lhd.nifs.ac.jp (M. Shoji).

0022-3115/$ - see front matter © 2004 Elsevier B.V. All rights reserved.
doi:10.1016/j.jnucmat.2004.10.041

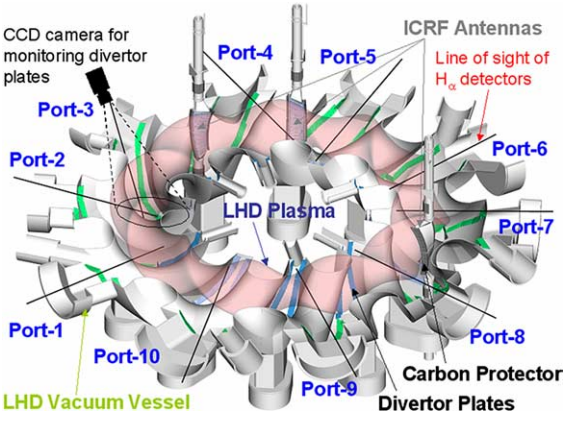

Fig. 1. Bird's eye view of the cross-section of the vacuum vessel with plasma heating and diagnostic systems for long pulse discharges by ICRF heating. The lines of sight of the H_α emission detectors mounted on all outer ports are also depicted.

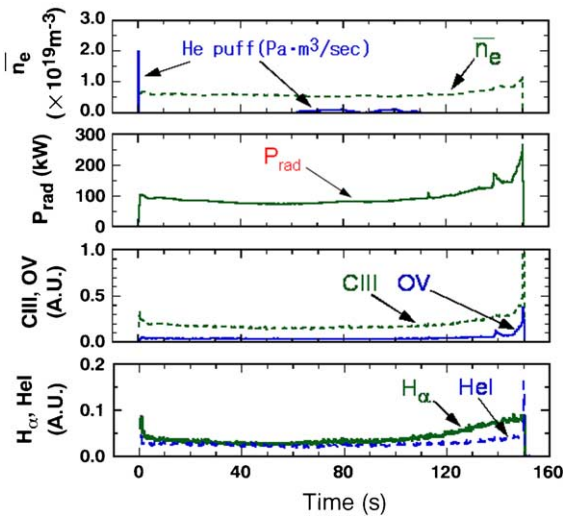

Fig. 2. Time evolution of typical plasma parameters (electron density n_e, radiation power P_{rad}, impurity radiation of CIII and OV and intensity of H_α and HeI) measured in the long pulse discharge.

layers are formed around the main plasma, and divertor plates (carbon) are installed on the vacuum vessel along strike points where plasma flow from the main plasma reaches to the vacuum vessel along magnetic field lines. Thermocouples are embedded in some divertor plates for temperature measurement [2].

Three pairs of ICRF antennas with carbon protectors are installed in port-3.5, 4.5 and 7.5. The antennas consist of upper and lower parts supported from the upper and lower ports, respectively. In the long pulse discharges, a minority heating method was employed in majority helium plasmas with hydrogen as the minority ions. The ion cyclotron resonance (ICR) layer was located at the saddle point of the mod-B surface for optimizing heating efficiency [3]. The toroidal distribution of neutral hydrogen has been measured with single channel H_α emission detectors mounted on all outer ports. A visible CCD camera mounted on an outer port (port-3) observed divertor plates and the divertor legs near a lower port (port-2.5).

3. Experimental results in a long pulse discharge by ICRF heating

We succeeded in sustaining the plasma for 150 s by ICRF heating [4]. The plasma parameters were as follows: the average electron density $n_e = 5\text{–}6 \times 10^{18}$ m^{-3}, the central electron and ion temperature T_{e0}–$T_{i0} \sim 2$ keV and the ICRF heating power $P_{ICRF} \sim 500$ kW. One pair of the ICRF antennas installed in port-3.5 was used in this discharge. The plasma was terminated by uncontrollable plasma density rise with gradual increase in the H_α intensity in the later phase of the discharge (after $t = 100$ s) as shown in Fig. 2.

The radiation power P_{rad} and impurity emission (CIII, OV) also exhibited similar time evolution. The increment in the H_α intensity is observable compared to that of impurities. Fig. 3 illustrates the toroidal distribution of the H_α intensity ratio $I_{H\alpha}^{150\,s}/I_{H\alpha}^{90\,s}$, where $I_{H\alpha}^{150\,s}$ and $I_{H\alpha}^{90\,s}$ are the intensity measured at $t = 150$ s and 90 s, respectively, showing a peaked profile around port-3, and yellow circles represent the temperature of the divertor

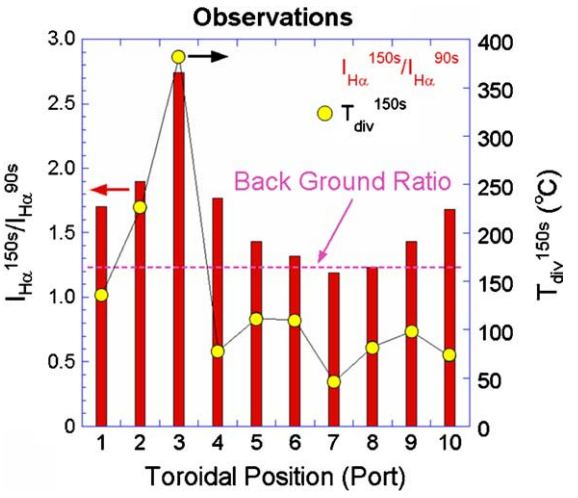

Fig. 3. Toroidal distribution of the ratio of the H_α intensity at 90 s and 150 s, and that of the divertor plate temperature installed near inner ports measured at 150 s (yellow circles).

plates installed near inner ports, which also exhibits local heating of the divertor plate installed at port-3. The CCD camera observed local heating (a hot spot) of a vertically installed divertor plate in port-2.5. These experimental results indicate that hydrogen outgas was locally induced by heating of the divertor plates around port-3 during the long pulse discharge.

4. Analyses of the proton trajectories accelerated by ICRF waves

We calculated the trajectories of protons accelerated by ICRF waves excited from the antennas installed in port-3.5 by using a full orbit analysis code. Fig. 4 gives the toroidal and poloidal distribution of the calculated strike points (red crosses and blue open circles) together with the observed incremental temperature of the divertor plates (colored squares). In this figure, the toroidal angle ϕ of 0° is the position where the plasma is horizontally elongated, and the poloidal angle θ of 0° means the outboard side of the torus. The distribution of the strike points is consistent with that of the incremental temperature of divertor plates, and the position of the vertically installed divertor plate locates on the area where the strike points are concentrated. We, thus, consider the following three possible sources of strong outgas around port-3:

Case 1 the vertically installed divertor plate in port-2.5, which is locally heated by the accelerated protons (hot spot),

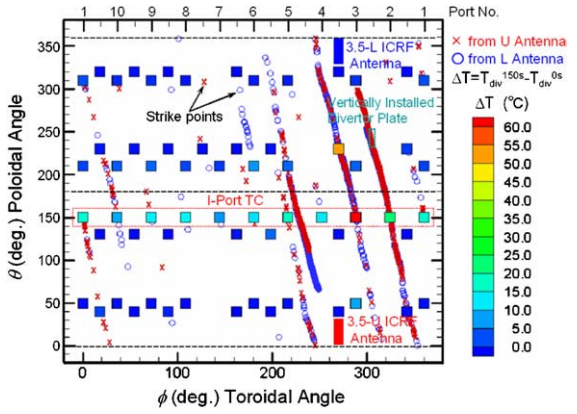

Fig. 4. The toroidal and poloidal distribution of the strike points of the accelerated protons by ICRF waves excited from the upper (red crosses) and lower antennas (blue open circles), and temperature increments of the divertor plates (colored squares) during the ICRF heating. The position of the ICRF antennas and the vertically installed divertor plate are also indicated.

Case 2 the protectors for the ICRF antenna heated by a RF current and a plasma heat load,

Case 3 divertor plates heated by the protons accelerated by the ICRF waves, which are toroidally and poloidally distributed along the strike points of the protons.

5. Three-dimensional neutral particle transport simulation

Density profiles of neutral hydrogen are computed by a neutral particle transport simulation code (DEGAS ver. 63) for the above three cases [5]. In the simulation, test particles representing neutral hydrogen are launched into a three-dimensional grid model for the LHD plasma configuration. The plasma parameter profiles in the grid model are determined on the basis of the measurements of plasma diagnostics (Thomson scattering for T_e, and a far infrared interferometer for n_e). We assumed that the ion temperature is identical to the electron temperature. The toroidal and poloidal distribution of the plasma parameters on the divertor legs are estimated from the measurements with a reciprocal Langmuir probe and the probes embedded in the divertor plates. We calculated the neutral density profile in the above three cases by changing the position and distribution of test particle emission. The test particles (neutral hydrogen molecules) are launched from the vertically installed divertor plate (case 1) and from the protector (case 2). In case 3, the test particles are released from toroidally and poloidally distributed divertor plates. Experimental results of a performance test on the divertor plates generally show linear dependence of the outgas rate on the divertor plate temperature (also on the heat flux) up to 400°. We, thus, defined the distribution of the test particle emission in case 3 as that of the heat flux on the divertor plates calculated by the proton trajectory analyses.

The calculations of the density profile of atomic hydrogen in the above three cases are shown in Fig. 5. Hydrogen atoms are locally concentrated near the vertically installed divertor plate (in case 1) and the protector (in case 2). The complicated shape of the LHD plasma and the vacuum vessel probably obstruct toroidal diffusion of the neutral particles. In case 3, the neutral atoms widely spread because of the toroidally distributed sources of the hydrogen outgas. The toroidal distribution of the H_α intensity in the three cases $\Delta I_{H\alpha}{}^{\text{by ICRF}}$ is obtained by integrating the calculated H_α emission along the line of sight of the detectors. Fig. 6 is the toroidal distribution of the H_α intensity, in which the intensity is normalized to that at port-3. In the observations of the toroidal distribution of the H_α intensity (shown in Fig. 3), we regard the average value of the ratio measured at port-6, 7 and 8 as a background ratio caused by usual plasma–wall interactions without the

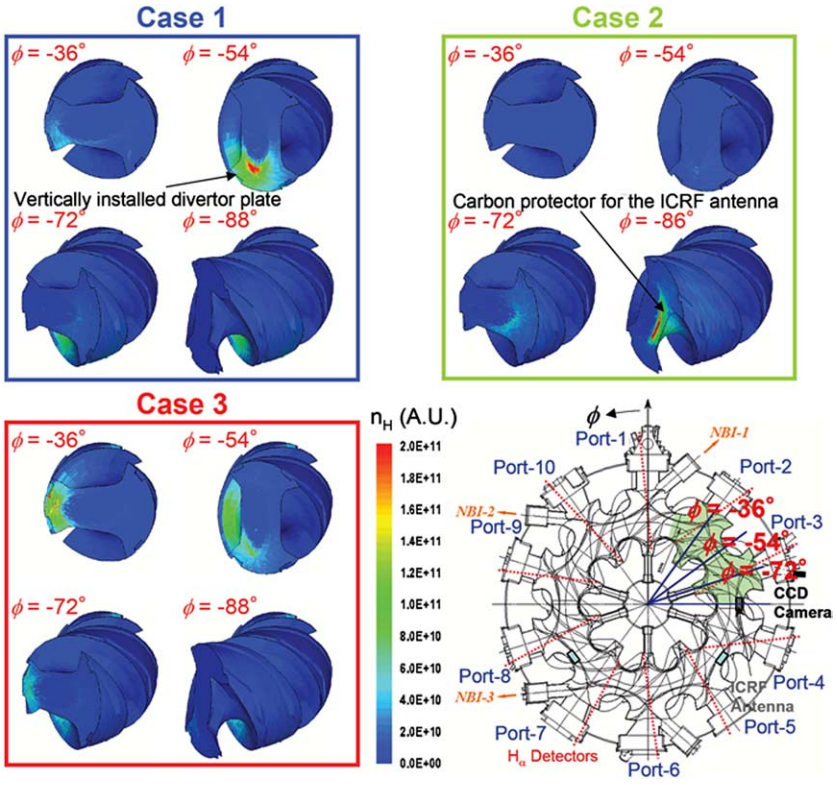

Fig. 5. The calculations of the three-dimensional density profile of atomic hydrogen in the grid model between port-2 and port-3 in the three different cases of the hydrogen outgas.

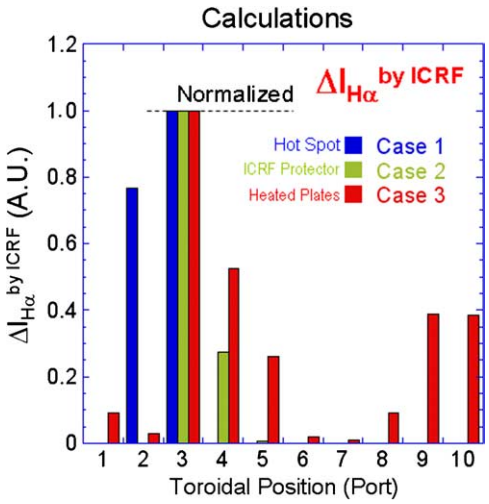

Fig. 6. Calculations of the toroidal distribution of the normalized H_α intensity in the three different cases of the hydrogen outgas.

effect of the accelerated protons. Comparison between the calculations and the observations (the background ratio should be subtracted) shows that the H_α intensity in case 1 and 2 is strongly peaked at port-3, which is not in agreement with the observations. The toroidally distributed sources of hydrogen outgas in case 3 can explain the observed toroidal distribution of H_α intensity rise in the long pulse discharge.

6. Conclusion

Uncontrollable plasma density rise occurred in the later phase of an ICRF heated long pulse discharge in LHD. Toroidally non-uniform increases of the divertor plate temperature and the H_α intensity were observed. The distribution of the temperature increase of the divertor plates is consistent with that of the strike points of accelerated protons by the ICRF waves. Neutral particle transport simulation shows that the hydrogen outgas from the divertor plates heated by the accelerated protons is necessary for explaining the observations of the H_α intensity rise. It strongly suggests that the reduction of outgas from the toroidally and poloidally distributed divertor plates installed along the strike points of the

accelerated protons is effective for sustaining long pulse discharges with control of the plasma density.

Acknowledgment

The authors gratefully acknowledge Professor O. Motojima for his encouragement. The author (M.S.) would like to thank technical officers in department of engineering and technical services in NIFS for their experimental support.

References

[1] O. Motojima et al., Phys. Plasmas 6 (1999) 1843.
[2] S. Masuzaki et al., J. Nucl. Mater. 240–243 (2001) 12.
[3] R. Kumazawa et al., Plasma Phys. Control. Fus. 45 (2003) 1037.
[4] K. Saito et al., these Proceedings. doi:10.1016/j.jnucmat.2004.10.140.
[5] D.B. Heifetz et al., J. Comput. Phys. 46 (1982) 309.